Foam Propagation at Low Superficial Velocity: Implications for Long-Distance Foam Propagation

Yu, Guanqun; Vincent-Bonnieu, S.; Rossen, Bill

DOI
10.3997/2214-4609.201900108

Publication date
2019

Document Version
Final published version

Published in
Proceedings of the 20th European Symposium on Improved Oil Recovery

IOR 2019
20TH EUROPEAN SYMPOSIUM ON IMPROVED OIL RECOVERY

EAGE

Tu A 10

Foam Propagation at Low Superficial Velocity: Implications for Long-Distance Foam Propagation

G. Yu[1]*, S. Vincent-Bonnieu[2], W. Rossen[1]

[1]Delft University of Technology; [2]Shell Global Solutions International B.V.

Summary

Since the 1980s experimental and field studies have found anomalously slow propagation of foam that cannot be explained by surfactant adsorption. Friedmann et al. (1994) conducted foam-propagation experiments in a cone-shaped sandpack and concluded that foam, once formed in the narrow inlet, was unable to propagate at all at lower superficial velocities towards the wider outlet. They hence concluded that long-distance foam propagation in radial flow from an injection well is in doubt.

Ashoori et al. (2012) provide a theoretical explanation for slower or non-propagation of foam at decreasing superficial velocity. Their explanation connects foam propagation to the minimum velocity or pressure gradient required for foam generation in homogeneous porous media (Gauglitz et al., 2002). The conditions for propagation of foam are less demanding than those for creation of new foam. However, there still can be a minimum superficial velocity necessary for propagation of foam, except that it could be significantly smaller than the minimum velocity for foam generation from an initial state of no-foam. At even lower superficial velocity, theory (Kam and Rossen, 2003) predicts a collapse of foam.

In this study, we extend the experimental approach of Friedmann et al. in the context of the theory of Ashoori et al. We use a cylindrical core with stepwise increasing diameters such that the superficial velocity in the outlet section is 1/16 of that in the inlet. N2 foam is created and stabilized by an alpha olefin sulfonate surfactant. Previously (Yu et al., 2019), we mapped the conditions for foam generation in a Bentheimer sandstone core as a function of total superficial velocity, surfactant concentration and injected gas fraction (foam quality). In this study, we extend the map to include the conditions for propagation of foam, after its creation in the narrow inlet section at greater superficial velocity. Thereafter, by reducing superficial velocity, we map the conditions for foam collapse.

Our results suggest that the minimum superficial velocities for foam generation, propagation and maintenance increase with increasing foam quality and decreasing surfactant concentration, in agreement with theory. The minimum velocity for propagation of foam is much less than that for foam generation, and that for foam maintenance is less than that for propagation. The implications of our lab results for field application of foam are discussed.

Introduction

Applications of foam in porous media range from enhanced oil recovery (EOR) (Schramm, 1994; Rossen, 1996) and acid diversion in well stimulation (Burman and Hall, 1987; Kennedy et al., 1992) to aquifer- and soil-remediation processes (Hirasaki et al., 1997). For petroleum reservoir engineers, foam EOR is of great interest since foam significantly improves the volumetric sweep efficiency of injected gas. Foam in porous media comprises liquid films (called lamellae) restricting the flow of gas in the pore network. The presence of lamellae greatly reduces gas mobility, resulting in improved gas sweep. The number of lamellae per unit volume of gas (inversely related to bubble size) determines the mobility reduction (also called the "strength") of foam. The population of lamellae, and therefore properties of the foam, is the result of processes creating and destroying lamellae.

Propagation of foam over long distances far from injection well is needed to divert gas flow deep into a reservoir. The conditions that dominate both creation and propagation of foam in porous media, therefore, have been one of the primary concerns to foam researchers for decades. Various theories and experimental results cast light on the mechanisms of foam generation and propagation.

Theory suggests that a minimum pressure drop ΔP^{min} is required to mobilize a static lamella blocking a pore throat (Bikerman, 1973; Rossen and Gauglitz, 1990). Mobilized lamellae can multiply by lamella division (Rossen, 1996) and repeated snap-off (Falls et al., 1988; Ransohoff and Radke, 1988), triggering foam generation. A percolation theory for foam generation in steady gas-liquid flow (Rossen and Gauglitz, 1990) relates the minimum pressure gradient ∇P^{min} or minimum superficial velocity u_t^{gen} for foam generation to rock and fluid properties such as permeability k, surface tension σ and injected liquid volume fraction f_w. This theory fits experimental data (Friedmann et al., 1994; Rossen and Gauglitz, 1990; Yu et al., 2019) regarding the impact of injected liquid fraction f_w on the minimum velocity for foam generation. A greater injected liquid fraction f_w contributes to lamella creation (Rossen and Gauglitz, 1990), and also reduces the rate of lamella coalescence (Khatib et al., 1988). Foam generation hence becomes easier as f_w increases because of effects on both lamella creation and destruction. More-recent work (Yu et al., 2019) indicates an effect of surfactant concentration on the minimum velocity for foam generation, which reflects the link between lamella stability and foam generation. The surfactant concentrations used in that study (Yu et al., 2019) are far above the critical micelle concentration (CMC) (Jones et al., 2016).

Gauglitz et al. (2002) conducted three different types of foam-generation experiments. In fixed-injection-rate experiments (Figure 1a), foam is generated by fixing total superficial velocity and foam quality (gas fractional flow, $f_g \equiv (1-f_w)$). Superficial velocity is first set at a low value and then is stepwise increased to greater values. Upon triggering of foam generation at u_t^{gen}, pressure gradient along the core rises abruptly (Gauglitz et al., 2002; Yu et al., 2019) to a much larger value reflecting strong foam. If superficial velocity is reduced after strong foam is created, the strong foam can be maintained at superficial velocities at which it would not be created from a state of no-foam or coarse foam.

In fixed-pressure-difference experiments (Figure 2a), foam is generated by maintaining the pressure drop across the core at a set value (Gauglitz et al., 2002) and increasing this pressure difference in steps. These experiments reveal a third steady state over a range of superficial velocities, with pressure gradient intermediate between the coarse-foam and strong-foam states. The values of ∇P^{min} and u_t^{gen} in an experiment at fixed injection rate correspond to the point where the plot of $u_t(\nabla P)$ bends backwards toward smaller values of u_t with increasing∇P.

The population-balance model of Kam and Rossen (2003) and its variants (Kam et al., 2007; Kam, 2008; Ashoori et al., 2012) are designed to explain the experiments of Gauglitz et al. (2002). This model introduces a relation between pressure gradient, lamella creation and foam generation. It is the only foam model demonstrated to represent and explain the trigger and multiple steady-states seen in foam-generation experiments (Gauglitz et al., 2002). Its predicted behaviour is shown schematically in Fig. 2b.

Successful foam propagation in the field resembles a radial flow pattern with stable displacement of gas due to mobility control at the gas-displacement front. In the near-well region, the high velocities of gas and liquid, as well as high pressure gradient, favour the generation and propagation of foam (Rossen and Gauglitz, 1990). At large distances away from an injection well, however, both superficial velocity and pressure gradient are low, and the issue of foam propagation further from the

well comes into question. Some field applications of steam foam in the 1980's reported very slow foam propagation to limited distances from the injector, and hence raise concerns about long-distance foam propagation. Observation wells in a steam-foam pilot in the Mecca Lease, Kern River, reported foam propagation to a distance 43 m from the injector over 4.5 years (Patzek, 1996). This was slower than the rate that would be predicted from surfactant adsorption and the high foam quality (injected gas fraction) in that test. In section 26 of the steam-foam pilot in the Midway-Sunset (MWSS) field, two observation wells 12 m (<40 ft) from the injector reported a breakthrough of steam foam after 8 months of surfactant injection (Friedmann et al., 1994; Patzek, 1996). Based on the estimated foam propagation rate to 12 m, foam should have arrived at the observation well 21 m (around 70 ft) from the injector after 24+ months of surfactant injection (Friedmann et al., 1994; Patzek, 1996). Unfortunately, surfactant injection continued for a period of only 18 months before it was shut off, and hence left the hypothesis untested (Patzek, 1996).

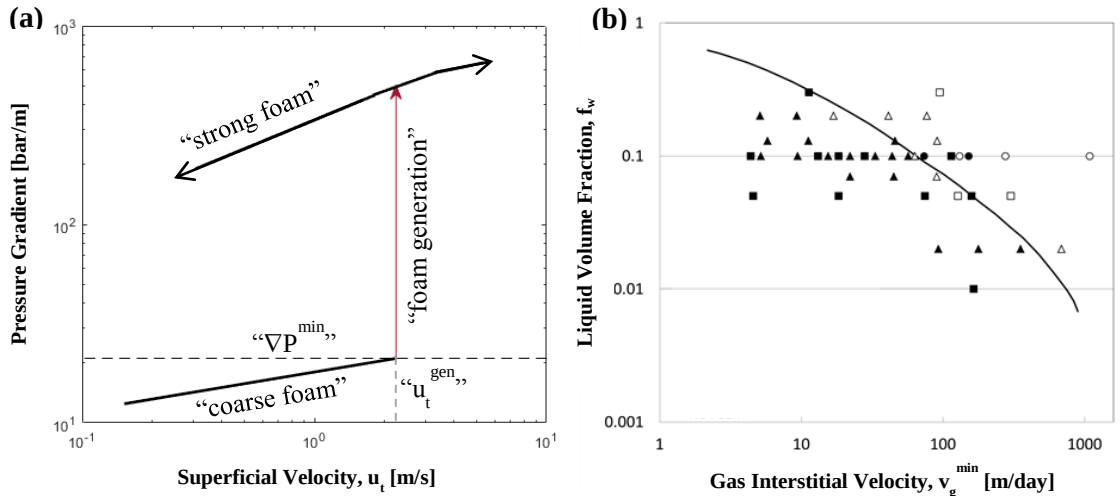

Figure 1 (a) *Schematic of fixed-injection-rate experiment on foam generation (Gauglitz et al., 2002). Foam generation in steady flow requires exceeding a minimum pressure gradient* ∇P^{min} *or minimum superficial velocity* u_t^{gen}. ***(b)*** *The minimum gas interstitial velocity for foam generation* v_g^{min} *at different injected liquid volume fractions. Closed symbols represent conditions with no foam, and open circles conditions with strong foam. The trend superimposed on data is estimated from a percolation-theory-based model for foam generation in steady flow in homogeneous porous media (Gauglitz et al., 2002).*

Friedmann et al. (1994) conducted a foam-propagation experiment in a cone-shaped sandpack to seek explanations for what they interpreted as failure of propagation of steam foam in the MWSS pilot. Surfactant (Chevron Chaser SD1020, 0.3 wt%) and N_2 were coinjected (at constant $f_g = 0.987$) from the narrow inlet of the cone-shaped sandpack (with a 1.25:5.00 ratio of injection-/exit-face diameters). Foam generated near the inlet section then propagated to increasingly wider downstream sections, with six pressure-difference measurements in total. According to the pressure response, strong foam stalled in the fifth section and didn't reach the end of the sand-pack, even after 300 pore volumes (PV) of foam injected.

In another study of foam propagation in a homogeneous porous medium, Friedmann et al. (1991) combined core-flooding experiments and numerical simulation. They developed a population-balance simulation model and fit the model's coefficients to the results of 6 separate core-flooding experiments. Afterwards, they conducted a foam-displacement experiment in a Berea sandstone core with three different, increasing diameters (0.95 cm, 2.5 cm, and 5.0 cm) along the core length, and compared the data to the simulation results of their population-balance model. Surfactant solution and N_2 were coinjected (at $f_g = 95\%$, and T = 100 ˚C) into the vertically mounted core at a velocity that creates strong foam only in the narrow section (d = 0.95 cm). Foam propagation in the widest portion (d = 5.0 cm) was then observed and documented based on the pressure-difference measurements across the three sections in the widest portion.

Their population-balance simulation model assumes a minimum velocity for lamella creation. Coalescence depends in the model on surfactant concentration but not on capillary pressure or water saturation. Their simulation and experimental results agree well with each other, and show that the breakthrough of strong foam at the core outlet was delayed by about 3.3 PV when compared to the breakthrough of surfactant. With a minimum velocity for lamella generation, the model should predict a minimum velocity for propagation and for maintaining foam, but this is not explored in the paper.

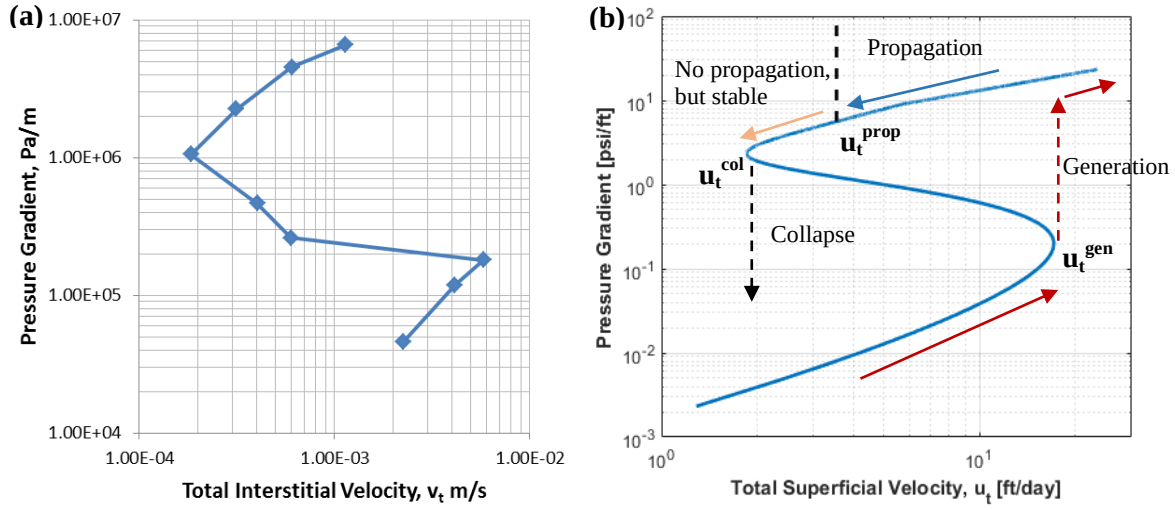

Figure 2 (a) *Data of Gauglitz et al. (2002) from a fixed-pressure-difference experiment on foam generation.* ***(b)*** *Illustration of the population-balance model of Kam and Rossen (Kam, 2008) fitted to the data from a different foam-generation experiment (Ashoori et al., 2012). In the example shown here, the critical superficial velocity for foam propagation at $f_w^J = 0.1$ is $u_t^{prop} = 3.55$ ft/day (Ashoori et al., 2012). Solid arrows illustrate the injection history of foam. Ashoori et al. investigated the value of u_t^{prop} for this model with these parameters, but not specifically u_t^{gen} or u_t^{col}.*

Ashoori et al. (2012) used the population-balance model of Kam and Rossen (2008) to explain and predict long-distance foam propagation in the context of multiple foam steady-states. They combined fractional-flow analysis (also called the method of characteristics) and numerical simulation to study long-distance foam propagation at various superficial velocities in a 1-D linear porous medium. At superficial velocities greater than the minimum velocity for generation u_t^{gen} (Rossen and Gauglitz, 1990; Gauglitz et al., 2002; Yu et al., 2019), strong foam can be created in-situ and propagate downstream (Figure 2b, red arrows). As superficial velocity decreases (Figure 2b, blue arrow), an intermediate state of weak foam propagates ahead of the strong-foam state, whose propagation rate slows. This may explain the delay in breakthrough of strong foam seen in Friedmann et al.'s (1991) experiment. With further reduction of superficial velocity to a minimum velocity for propagation, which we here call u_t^{prop}, the characteristic velocity of strong foam drops to zero; foam stops moving forward (Figure 2b, blue arrow). The model indicates that, however, strong foam remains stable in place at u_t^{prop} (Figure 2b, yellow arrow). At a yet-lower superficial velocity u_t^{col}, foam becomes unstable and collapses (Figure 2b, black arrow). Their analysis implies that the failure of foam propagation at u_t^{prop} is a result of insufficient lamella creation at the leading edge of foam front (from insufficient pressure gradient there), instead of complete destruction/collapse of foam. In other words, the flux of lamellae to the foam displacement front is quenched by the rate of lamella coalescence at the front.

In this study, we focus on gathering experimental evidence on foam propagation in a core of variable diameter. The configuration of this core (Figure 4), based on that originally designed by Friedmann et al. (1991), provides an opportunity for foam to flow at three different superficial velocities u_t in three core sections of different diameter as it is injected at a constant volumetric flow rate Q_t. As described above, Ashoori et al.'s analysis (2012) suggests the existence of three transition points for foam behaviour in terms of superficial velocity, illustrated schematically in Fig. 2b: u_t^{gen},

the minimum velocity for foam generation; u_t^{prop}, the minimum velocity for foam propagation; and u_t^{col}, the velocity below which steady-state strong foam becomes unstable and collapses. We therefore design our experimental procedures (described below) in a way that the model's implications (Ashoori et al., 2012) can be examined and verified. Furthermore, we also explore the impacts of surfactant concentration C_s and foam quality f_g (plotted in terms of injected liquid volume fraction f_w below) on long-distance foam propagation. We plot the three key velocities (u_t^{gen}, u_t^{prop}, and u_t^{col}) against different foam qualities and surfactant concentrations. We then analyse the trend of data and discuss the implications.

In field applications, surfactant solution and gas are frequently injected in alternating slugs ("SAG" injection). In the near-well region, alternating drainage and imbibition creates beneficial conditions for foam generation, more favourable than in steady flow. At distances far away from injection well, however, the effects of alternating slug injection are damped; fractional flow is expected to be more steady. In our experiments, surfactant and N_2 are coinjected at a fixed liquid volume fraction, a condition that we believe resembles the conditions far from an injection well in even a SAG process.

Experiment apparatus and materials

Figure 3 is a schematic of the apparatus. The core is mounted vertically, with the narrow section at the bottom. Surfactant solution or brine and N_2 are coinjected from the bottom. In total 7 pressure transducers (0~150 bar) and 6 pressure-difference meters (0~10 bar) are placed along the core to monitor foam propagation. We use a cylindrical core of Bentheimer sandstone (k = 2.5 Darcy, $\boldsymbol{\Phi}$ = 0.25) with stepwise changing diameters (Figure 4). All experiments are conducted at a lab temperature of approximately 22˚C. Surfactant solutions are made by weighing and mixing BIO-TERGE AS-40 (C14-16 Alpha Olefin Sulfonate) in brine (3.0 wt% NaCl). The vertically mounted core is divided into three sections (Figure 4): 1) a narrow inlet Section 1 at the bottom, with diameter 1 cm and length 6.1 cm (pore volume (PV) ≅ 1.2 ml); 2) a wider middle Section 2 with diameter 2.67 cm and length 6.9 cm (PV ≅ 9.7 ml); and 3) the widest and longest Section 3, with diameter 4 cm and length 27.0 cm (PV ≅ 84.8 ml). The ratio of superficial velocities is 16.0:7.1:1.0 from Section 1 to Section 3. The core is drilled from one large piece of cylindrical core (40 cm long and 4 cm wide) to avoid capillary discontinuities. Figure 4 illustrates the locations of the pressure gauges along the core. A constant back-pressure of 40 bar is applied during the experiments.

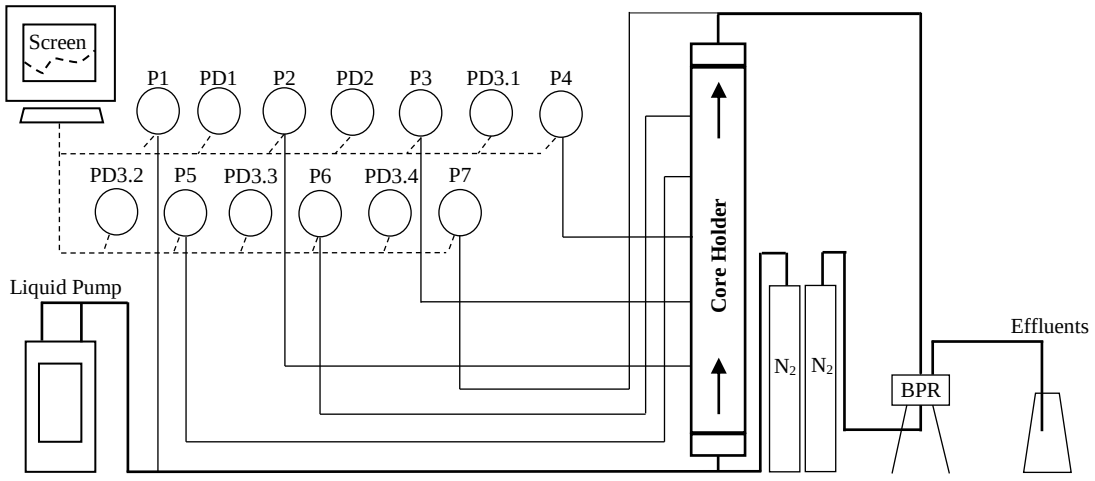

Figure 3 *Apparatus design. The core is mounted vertically with the narrow section at the bottom. Liquid and N_2 are coinjected from the bottom. In total, 7 pressure transducers P (range 0~150 bar) and 6 pressure-difference meters DP (0~10bar) are placed along the core to monitor foam propagation.*

The pressure transducers used in our experiment are placed some distance from the section boundaries (Figure 4): ΔP_1 measures the pressure drop across Section 1 and the first half of (about 3.5 cm) of Section 2; ΔP_2 measures the second half of Section 2 and the beginning (about 3.0 cm) of

Section 3. Drilling holes directly at the section boundary would be difficult, and distortion in flow at the boundary is difficult to interpret. We can infer the presence of strong foam in Section 1 from a large pressure difference between the first two taps ΔP_1; propagation through second Section 2 from the pressure difference between the second and third taps ΔP_2; and propagation the widest section, Section 3, from the next three pressure differences, ΔP_3, ΔP_4, and ΔP_5 (Figure 4). The pressure difference in near the outlet ΔP_6 could be distorted by the capillary end effect. We are most interested in propagation in the downstream section (Section 3).

To accommodate the range of our mass-flow controller, back-pressure had to be varied among experiments. Back-pressure was greater than 10 bar in all experiments, and was held constant in each experiment (i.e., for all data at each foam quality and surfactant concentration), with one exception. In one case upstream pressure approached the safety limit of the apparatus after foam propagation was demonstrated in Section 3. In that case, we reduced back-pressure somewhat and re-established steady-state strong foam throughout the core before proceeding to measure the velocity for foam collapse. While gas compression, even with the BPR in place, affects superficial velocity and foam quality near the inlet, at all times we are interested in generation, propagation or collapse of foam at the foam front, with no foam downstream of it. Therefore, these results are not significantly affected by gas compression along the core.

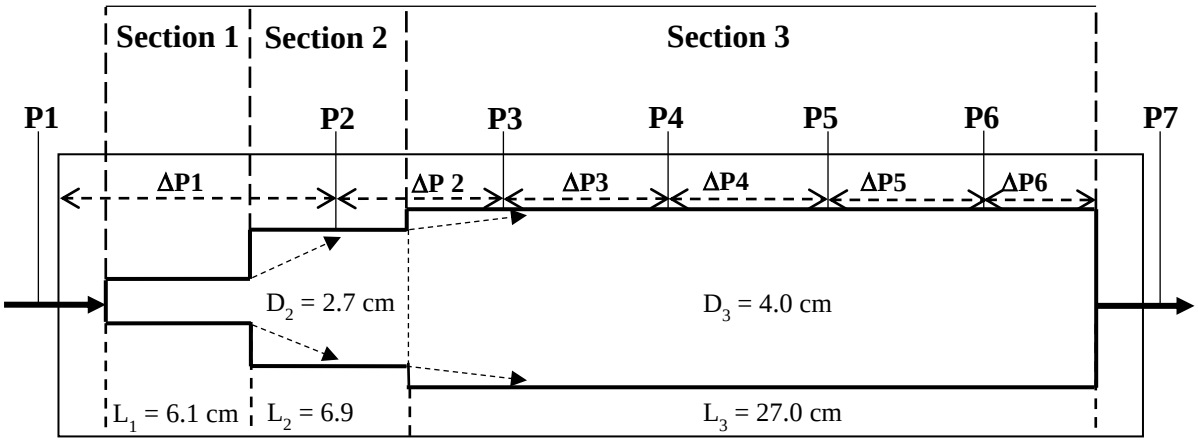

Figure 4 *Schematic illustration of core geometry.*

Experimental method: defining criteria and procedure

Analogous to the criteria defined by Yu et al. (2019) for foam-generation experiments, we define here the criteria and procedures for foam-propagation experiments. The experiments proceed in three steps designed to determine the conditions for foam generation in Section 1, and then for propagation in Sections 2 and 3, and finally for foam collapse in Sections 3 and 2.

Determination of the minimum velocity for foam generation u_t^{gen}: The first series of steps (steps 1 to 3) is designed to measure u_t^{gen} in Section 1, and establish a base before propagation into Sections 2 and 3. The criteria for determining u_t^{gen} are taken from Yu et al. (2019). A steady state of low ΔP_1 must first be established. Then superficial velocity is raised until, upon such an increase, ΔP_1 rises quickly to a much-larger value, signalling foam generation.

1. To determine u_t^{gen} in the given experiment, start with an injection rate well below the expected value of u_t^{gen}. If u_t^{gen} for a particular surfactant concentration and liquid volume fraction is already known or can be estimated from available data, one can use that information to select and initial injection rate of surfactant and gas. If an estimate of u_t^{gen} is not available, start at a relatively low a value of superficial velocity in Section 1.
2. Initialize the core with steady flow of brine and N_2 at this superficial velocity.
3. Start co-injection of surfactant solution and N_2 at this same superficial velocity and liquid volume fraction f_w. Since the pore volume of the Section 1 is about 1.2 ml, keep the injection rate constant until at least 2.0 to 3.0 ml of surfactant is injected, to satisfy adsorption in in that

section. If no foam generation is indicated (no substantial increase in ΔP_1), increase the injection rate in steps until foam generation is indicated by a sharp rise in ΔP_1 by at least a factor or 10, well beyond the magnitude of the increase in superficial velocity. As noted below, it is usually not possible to allow ΔP_1 to reach steady state before reducing injection rate to prepare for the next step. If foam is already indicated by a large value of ΔP_1 at the first injection rate, then u_t^{gen} cannot be determined from this experiment; the minimum velocity for generation may be less than the initial value tested. The test for propagation can continue, however. The uncertainty in u_t^{gen} is the gap between the last superficial velocity before foam generation and the superficial velocity at which foam generation occurred.

Determination of the minimum velocity for foam propagation u_t^{prop}: Propagation of foam to the next section (steps 4 to 8) is indicated by a rise in the next sectional ΔP by up to a factor of 100. The next series of steps are designed to determine u_t^{prop} from ΔP data from Sections 2 and 3 in turn, as follows:

4. After foam generation has occurred in Section 1, allow ΔP_1 to rise to between 4 and 5 bar. Before any significant increase is seen in ΔP_2, reduce injection rate to a much-smaller value, one that is not expected to allow propagation in Section 2. If ΔP_1 does not stabilize while there is a modest, steady value ΔP_2, it is not possible to determine u_t^{prop} in Section 2 in this experiment; foam propagation may already have occurred through Section 2. (In that case, go to step 6 if desired to check propagation into Section 3, but first verify that propagation does not proceed immediately into Section 3.) If propagation is not indicated in Section 2 at the first superficial velocity, continue with the low injection rate for a long period (~24 hr) before any further changes, to verify that propagation of strong foam has not occurred into Section 2.
5. If no strong foam is indicated in Section 2 after a long period of injection (~24 hrs), raise superficial velocity in a series of steps to greater values, and after each step keep the injection rate constant for a relatively short period of time. Repeat this procedure until strong foam is indicated in Section 2 by a rise in ΔP_2. The first indication of propagation in Section 2 is a steady, large rise in ΔP_1, which should begin shortly after the increase in superficial velocity. (ΔP_1 comprises a significant part of Section 2). As ΔP_1 stabilizes, ΔP_2 should start to rise and come to a value up to 100 times its earlier value. One should avoid waiting too long for the initial rise in pressure, to avoid the so-called "incubation effect," where slow accumulation of perturbations over long period co-injection of gas and surfactant solution can lead to foam generation under conditions in which it would not otherwise be seen (Baghdikian and Handy, 1990))
6. This superficial velocity is u_t^{prop} as measured in Section 2. From this superficial velocity estimate the injection rate at the inlet required for foam propagation in Section 3.
7. After a steady-state ΔP_2 is obtained, increase injection rate to a value somewhat lower than the injection rate for propagation in Section 3 estimated in the previous step. Verify that foam does not propagate at this velocity into Section 3 (i.e., ΔP_2 does not rise more than proportionately to the increase in injection rate, and ΔP_3 remains low).
8. If no foam is indicated in Section 3 in 1 to 2 hr, raise superficial velocity in a sequence of steps (each lasting approximately 1~2 hours) until foam is indicated by a rise in ΔP_3. The first indication of propagation to Section 3 is a steady, large rise in ΔP_2 from its previous steady value. Hold that injection rate constant until steady-state strong foam is established throughout the downstream portion of the core (i.e., in ΔP_4, ΔP_5, and ΔP_6). If foam does not propagate throughout the downstream portion of the core, raise velocity again in steps until it does. This final value represents u_t^{prop} for Section 3. We exclude any cases where a large pressure gradient at the end of the core, which reflects at least in part the capillary end effect, propagates upstream from the outlet (Ransohoff and Radke, 1988; Apaydin and Kovscek, 2001; Nguyen et al., 2003; Simjoo et al., 2013).

The uncertainty in u_t^{prop} for both Sections 2 and 3 is the gap between the largest velocity for which foam propagation is not indicated and the first velocity for which it is.

Determination of the velocity below which foam collapses u_t^{col}: Once foam is established throughout the core, collapse of foam in a given section (steps 9 to 12) is indicated when, upon a modest reduction in injection rate, there is an abrupt decrease in pressure difference in that section by a factor of 5 to 10. This reduction of pressure difference should be complete in a relatively short period (roughly 2~5 hours). It is likely that this represents a transition to continuous-gas foam (Fall et al., 1988; Rossen, 1996) instead of disappearance of all foam lamellae. We proceed as follows:

9. After the core is filled with strong foam, reduce superficial velocity in Section 3 in steps. The magnitude of velocity reductions should not be smaller than the velocity steps used in steps 5 to 8.
10. Hold the injection rate constant for at least 2 to 3 hr, to see whether or not the state of strong foam is maintained.
11. Collapse of strong foam is indicated by a reduction of pressure difference by a factor of 5 to 10 in Section 3. If foam collapse is indicated in Section 3, record this velocity as the minimum velocity to maintain strong foam, u_t^{col}. If strong foam remains stable, keep reducing velocity in steps until foam collapse is indicated (or until further reductions are not feasible with the apparatus). The uncertainty u_t^{col} is the difference between this velocity and the previous velocity tested.
12. Repeat steps 9 to 11 for Section 2. Document the value of u_t^{col} for Section 2 in the same way as for Section 3.

In case any of these procedures or criteria is violated, it may not be possible to record the desired velocity for the given section. We illustrate application of this experimental approach in the following section. As indicated in the examples in the next section, and reflected in Fig. 1b, there is some scatter in results from test to test, and sometimes judgments must be made in the application of our criteria.

Application of experimental methods

In this section, we illustrate application of our experimental method and the way we interpret some of the experimental complications. The vertical solid lines in Figures 5, 6, and 7 below represent times when superficial velocity is increased or reduced. The coloured curves represent the measured pressure differences between individual pairs of pressure taps. Figure 5 shows an experiment to measure u_t^{gen} in Section 1, specifically an experiment with f_g = 9% and C_s = 0.3 wt%. We start the test with co-injection of brine and N_2 at u_t = 22.21 ft/day in Section 1 (not shown). After steady-state is reached, we switch to co-injection of surfactant solution and N_2 (at the same u_t) at time zero in Fig. 5. Through successive increases in superficial velocity (221 ft/day, 228 ft/day, and 251 ft/day), strong-foam generation is triggered at u_t^{gen} = 251 ft/day at t = 1.4 hr (Figure 5a). Before foam reaches steady state in Section 1, we reduce superficial velocity to 13.32 ft/day and hold it constant for approximately 20.5 hours (Figure 5b), to verify that propagation of strong foam into Section 2 has not occurred. Pressure difference across Section 1 continues to increase, despite the reduced superficial velocity, and gradually stabilizes. Clearly there had been some reduction in mobility in Section 1 (rise in ΔP_1) upon the increase in u_t to 221 ft/day at about 0.9 hr, but it stabilized at a ΔP value too low to be considered strong foam. We conclude that u_t^{gen} is 251 ft/day in this experiment.

At t = 16.1 hr, ΔP_2 starts to rise, but then stabilizes at a value we judge too small to represent successful propagation of strong foam. At about 22 hr an increase in velocity triggers foam propagation in Section 2. Our next example focuses on a different experiment to illustrate the determination of u_t^{prop}.

Figure 6 shows an experiment with f_g = 95% and C_s = 0.05 wt% to illustrate the procedures for determining foam propagation in Sections 2 and 3. After foam generation is triggered Section 1 (not shown), we keep the superficial velocity steady at u_t = 11.4 ft/day for approximately 18 hours. There is no significant increase of ΔP_2, ΔP_3, or ΔP_4 during this period. We begin by raising superficial velocity in Section 2. For the first two superficial velocities tested (3.1 ft/day from 19.1-21.7 hr and 4.6 ft/day from 21.7-22.9 hr), no significant increase in either ΔP_1 or ΔP_2 is observed (Figure 6a). At 22.9 hr, we increase the superficial velocity to 6.2 ft/day. ΔP_1 immediately starts to increase (Figure 6a), indicating that strong foam begins to propagate into the first half of Section 2. After approximately 1.5 hr, ΔP_1 stabilizes, and at about the same time ΔP_2 starts a sharp and continuous increase to a value about 400 times greater than it had been. The sharp increase of ΔP_1, followed by

the increase of ΔP_2 to a much greater value, indicates the propagation of strong foam in Section 2 at u_t = 6.2 ft/day.

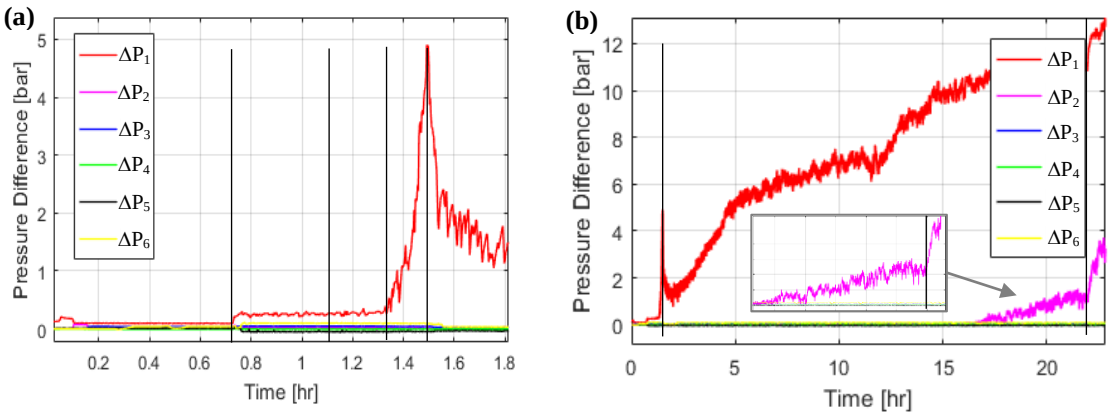

Figure 5 *Illustration of the experimental procedure for determining foam generation in Section 1 with f_g = 95% and C_s = 0.3 wt%.* ***(a)*** *Foam generation is triggered at 251 ft/day.* ***(b)*** *Superficial velocity in Section 1 is reduced to 13.32 ft/day after foam generation (at about 1.5 hr), to prevent immediate propagation of strong foam into Section 2, and held constant for around 20.5 hours. The vertical solid lines mark the moment of velocity increase. The inset is an enlarged view of ΔP_2 between about 17 and 23 hr.*

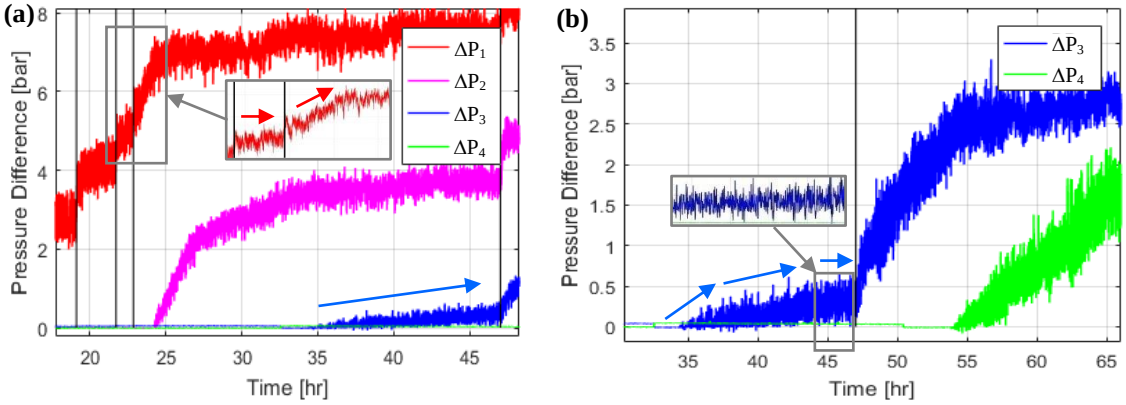

Figure 6 *Illustration of the experimental procedure for discerning foam propagation in Sections 2 and 3 with f_g = 95% and C_s = 0.05 wt%. Insets are enlarged views of the portions of the plots indicated by the boxes. Vertical lines represent times at which velocity increases.*

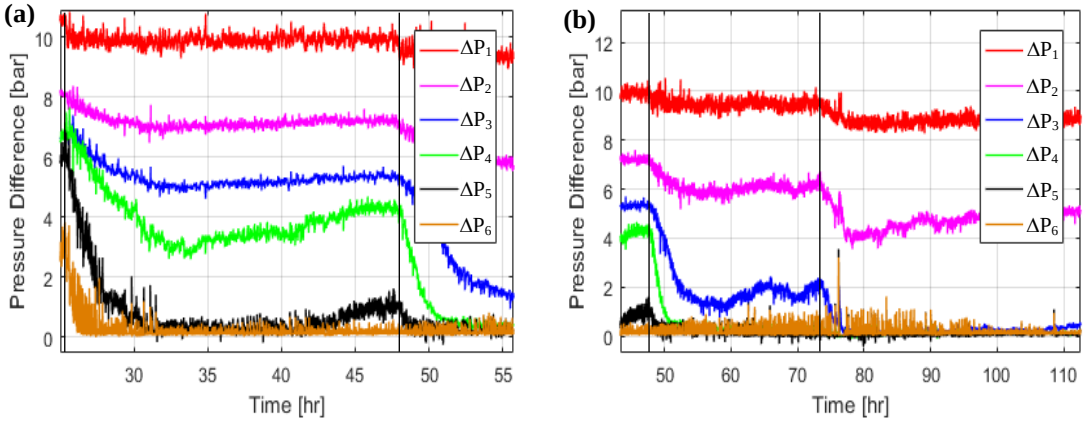

Figure 7 *Illustration of experimental procedures for determining foam collapse. f_g = 82 %, C_s = 0.05 wt%. Vertical lines represent times at which velocity decreases.*

We next repeat the same procedure for Section 3. As strong foam in Section 2 achieves steady state (at 34.5 hr), there is some increase of ΔP_3 (Figure 6a and 6b). ΔP_3 fluctuates between 0 and 0.5 bar for 13 hours (Figure 6b); eventually the trend stops increasing. This is similar to behaviour in Section 2 (ΔP_2) in the experiment in Figure 5b. In both cases, we judge that this does not indicate successful propagation of strong foam. Upon an increase in superficial velocity to 2.86 ft/day at about 46 hr, there is an unmistakable rise in ΔP_3. Moreover, foam propagates at this superficial velocity to ΔP_4 and further downstream (not shown). We judge u_t^{prop} to be 2.86 for Section 3 based on this result.

As noted, based on our criteria, a modest and stable increase in ΔP in a section is insufficient evidence for successful foam propagation. In addition, there is some inconsistency in results for Sections 2 and 3. For the experiment with f_g = 95% and C_s = 0.3 wt% (Figure 5b), propagation of strong foam begins at 2.94 ft/day in Section 2 and 1.94 ft/day in Section 3 (not shown). For the experiment with f_g = 95%, and C_s = 0.05 wt% (Figure 6), propagation of strong foam begins at 6.2 ft/day in Section 2 and 3.57 ft/day in Section 3. We report both results in our plots below.

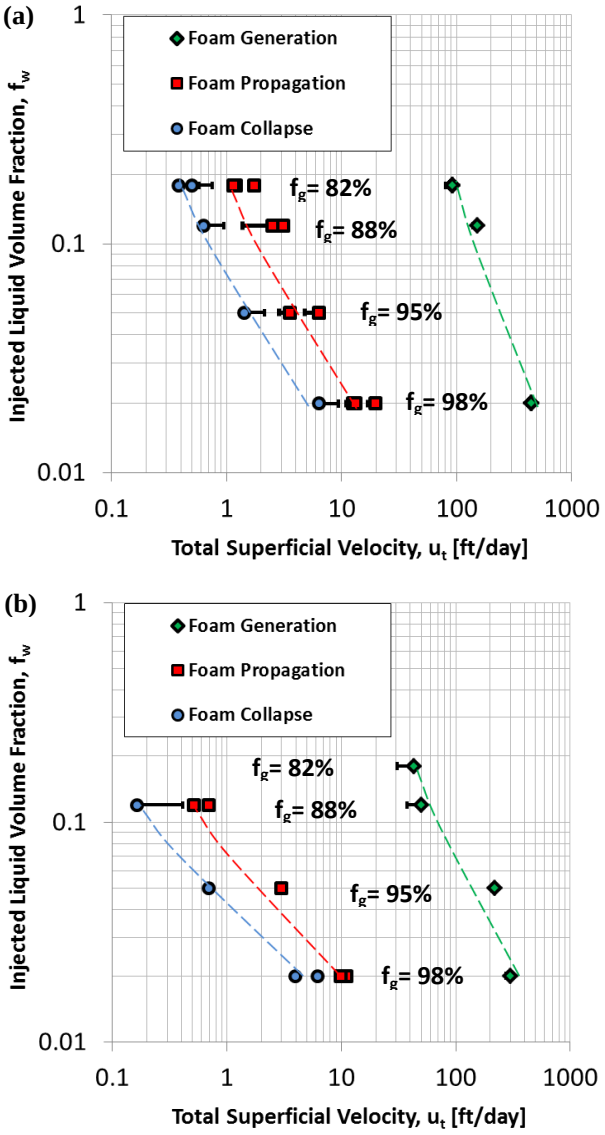

Figure 8 *Superficial velocities for generation, propagation, and destruction of foam. Values of u_t^{gen} are plotted in green, u_t^{prop} in red, and u_t^{col} in blue.* ***(a)*** *Experimental data for surfactant concentration C_s = 0.05wt%.* ***(b)*** *Experimental data for C_s = 0.3 wt%. The bars represent the difference between the next highest or lowest superficial velocity and the value at which generation, propagation or collapse were determined to have occurred. In some cases, this difference is too small to be visible here.*

In Figure 7, we illustrate the procedures for determining u_t^{col} for an experiment with f_g = 82% and C_s = 0.05 wt%. Strong foam propagates to Section 3 at 1.15 ft/day. At t = 25.4 hr, superficial velocity in Section 3 is reduced to 0.72 ft/day (Figure 7a). ΔP_5 and ΔP_6 start to drop, and fall below 1.0 bar in 5 hours (Figure 7a). ΔP_3 and ΔP_4 also start to drop, but eventually stabilize, and ΔP_3 even rebounds (Figure 7a). We further reduce superficial velocity to 0.58 ft/day at t = 47.8 hr (Figure 7a and 7b). ΔP_4, ΔP_5, and ΔP_6 drop below 1bar in about 4 hours, while ΔP_3 lingers at about 1.5 bar for another 23 hours. At t = 73.6 hr, we reduce superficial velocity Section 3 to 0.48 ft/day. ΔP_3 falls below 1.0 bar in 3 hours, indicating complete destruction of foam in Section 2. While there is some ambiguity in the exact value of u_t^{col}, we conclude that, for Section 3, u_t^{col} is 0.48 ft/day.

Summary of experimental results

In Figure 8, we plot the critical superficial velocities for foam generation, propagation and collapse against liquid fractional flow for two surfactant concentrations. We could not determine u_t^{prop} and u_t^{col} at the lowest foam quality for C_s = 0.05 wt% because of limitations on our mass-flow controller. The values of u_t^{prop} and u_t^{col} are considerably lower than u_t^{gen} for each surfactant concentration and foam quality (Figure 8). Although, as noted above, there is some scatter in results and some ambiguity in the determination of generation, propagation and collapse events, the distinction in magnitudes of the three velocities for each foam quality is clear. The results at the two surfactant concentrations are similar for foam generation and for propagation and collapse f_g = 0.98. Under wetter conditions (f_g = 0.88) foam propagates and remains stable at lower superficial velocities with the higher surfactant concentration. There uncertainty introduced by the stepwise increase/decrease of superficial velocity is indicated by the error bar for each datum in Figure 8. The leftward error bars represent the size of the last velocity increase for u_t^{gen} and u_t^{prop}. The rightward error bars represent the size of velocity reduction in determining u_t^{col}.

The dashed lines connecting the critical superficial velocities divide the data into four regions (Figure 8). The region to the right of the green dashed line represents conditions at which foam generation can occur in steady flow. The region between the green and red dashed lines defines conditions sufficient for foam propagation but not generation from a state of no-foam. The region between the red and blue dashed lines represents the conditions at which strong foam does not propagate but can be maintained in place. The region to the left of the blue dashed line represents conditions where foam can neither be generated nor maintained in steady flow for the given foam quality and surfactant concentration.

Conclusions

Our experiments confirm the existence of three critical superficial velocities for generation (u_t^{gen}), propagation (u_t^{prop}) and destruction (u_t^{col}) of foam in homogeneous porous media under steady flow conditions. Consistent with previous theory (Ashoori et al., 2011; 2012) and experiment (Friedmann et al., 1994), mobilizing strong foam requires a minimum superficial velocity u_t^{prop}. At superficial velocities less than u_t^{prop}, strong foam cannot propagate forward, but can be maintained in place until a yet-lower superficial velocity u_t^{col} is reached.

The critical superficial velocities needed to maintain the stability and the propagation of strong foam are considerably smaller than the superficial velocity required for triggering of foam generation at steady flow. Increasing surfactant concentration helps foam propagation and foam maintenance, most visible in our results under less-dry conditions.

As in previous studies (Rossen and Gauglitz, 1990; Gauglitz et al., 2002; Yu et al., 2019), foam generation becomes easier with increasing surfactant concentration (even far above the CMC) and increasing liquid volume fraction. The same trend applies for foam propagation and foam maintenance. Both liquid fraction and surfactant concentration are related to lamella stability, while superficial velocity is related to lamella creation. Both processes are important for foam generation, propagation and maintenance in place.

In our experiments, foam is generated and flows at low temperature (averagely 22˚C) and relatively low salinity (3.0 wt% NaCl). The porous medium used in our corefloods is homogeneous, free of oil, and highly permeable (which also indicates relatively low capillary pressure). Under

reservoir conditions (much greater temperature and salinity, lower permeability, presence of oil, in addition to many other complications), however, the difficulty of foam propagation observed in our experiments is likely to be magnified and occur at greater surfactant concentrations and greater velocities than measured in this study.

Acknowledgements
This project is supported the Joint Industry Project on Foam for EOR at Delft University of Technology. We thank and acknowledge both the sponsorship and advice of sponsoring companies and their representatives. Sebastien Vincent-Bonnieu gratefully acknowledges Shell Global Solutions International B.V. for granting the permission to publish this work. In addition, we thank Michiel Slob and Jolanda van Haagen Donker for their technical assistance with our experiments.

References
Ashoori, E.; Marchesin, D.; and Rossen, W.R.: Multiple Foam States and Long-Distance Foam Propagation in Porous Media. 2012, SPE Journal 17, 1231-45.
Apaydin, O.G. and Kovscek, A.R.: Surfactant Concentration and End Effects on Foam Flow in Porous Media. 2001, Transport in Porous Media 43, 511-536.
Baghdikian, S. and Handy, L.L.: Flow of Foaming Solutions in Porous Media. **1990**. *Modification of Chemical and Physical Factors in Steam-flood to Increase Heavy Oil Recovery.* Yortsos, Y.C., U. S. Dept. Energy Ann. Rep., DOE/BC/14126-14, Bartlesville, OK.
Burman, J.W. and Hall, B.E.: Foam Diverting Technique Improved Sandstone Acid Jobs. *Proc*., World Pet. Cong., New Orleans (1987).
Falls, A. H. Hirasaki, G. J., Patzek, T. W., Gauglitz, D. A., Miller, D. D., and Raulowski, T.: Development of a Mechanistic Foam Simulator: The Population Balance and Generation by Snap-Off. 1988, SPERE 3, 884-892.
Friedmann, F.; Chen, W.H.; Gauglitz, P.A.: Experimental and simulation study of high-temperature foam displacement in porous media. 1991, SPERE 6(1), 37–45.
Friedmann, F.; Smith, M.E.; Guice, W.R.; Gump, J.M.; Nelson, D.G. Steam-foam mechanistic field trial in the midway-sunset field. 1994, SPERE 9(4), 297–304.
Gauglitz, P.A.; Friedmann, F.; Kam, S.I. and Rossen, W.R.: Foam Generation in Homogeneous Porous Media. 2002. Chem. Eng. Sci. 57, 4037-4052.
Hirasaki, G.; Miller, C.; Szafranski, R.; Tanzil, D.; Lawson, J.B.; Meinardus, H.; Jin, M.; Londergan, J.T.; Jackson, R.; Pope, G.A.; Wade, W.H.: "Field Demonstration of the Surfactant/Foam Process for Aquifer Remediation." 1997. DOI:10.2523/39292-MS.
Jones, S. A.; Laskaris, G.; Vincent-Bonnieu, S.; Farajzadeh, R. and Rossen, W. R. Effect of Surfactant Concentration on Foam: From Coreflood Experiments to Implicit-Texture Foam-Model Parameters. 2016, J. Ind. & Eng. Chem. 37, 268-276.
Kam, S.I. and Rossen, W.R. A Model for Foam Generation in Homogeneous Media. 2003, SPE J. 8(4): 417-42,. SPE-87334-PA.
Kam, S.I.; Nguyen, Q.P.; Li, Q. and Rossen, W.R. Dynamic Simulations With an Improved Model for Foam Generation. 2007, SPE 35-38.
Kam, S.I. Improved Mechanistic Foam Simulation with Foam Catastrophe Theory. 2008, Colloids Surf., A 318 (1-3): 62-77.
Kennedy, J.W.; Kitziger, F.W.; and Hall, B.E.: Case Study on the Effectiveness of Nitrogen Foams and Water-Zone Diverting Agents in Multistage Matrix Acid Treatments. *SPEPE (May 1992) 203*.
Khatib, Z.R.; Hirasaki, G.J. and Falls, A.H. Effects of Capillary Pressure on Coalescence and Phase Mobilities in Foams Flowing Through Porous Media. 1988, SPE Res Eng 3 (3): 919-926. SPE-15442-PA.
Nguyen, Q. P.; Currie, P. K. and Zitha, P. L. J. Determination of Foam Induced Fluid Partitioning in Porous Media Using X-Ray Computed Tomography. 2003, Paper SPE80245 presented at the International Symposium on Oilfield Chemistry, Houston, TX, USA, 5-8.
Patzek, T. W.: Field Applications of Steam Foam for Mobility Improvement and Profile Control. 1996. Society of Petroleum Engineers. doi:10.2118/29612-PA
Ransohoff, T.C. and Radke, C.J. Mechanics of Foam Generation in Glass Bead Packs. 1988, Soc. Pet. Eng. Reservoir Eng., 3, 573.

Rossen, W.R. and Gauglitz, P.A. Percolation Theory of Creation and Mobilization of Foams in Porous Media. 1990, AIChE J. Vol. 36, No. 8.

Rossen, W.R. Foams in Enhanced Oil Recovery. In: Prud'homme, R.K., Khan, S. (Eds.), Foams: Theory Measurement and Applications. 1996, Marcel Dekker, New York City.

Simjoo, M. and Zitha, P. L. J. Effects of Oil on Foam Generation and Propagation in Porous Media. 2013, Paper SPE 165271 presented at the SPE Enhanced Oil Recovery Conference, Kuala Lumpur, Malaysia, 2-4.

Yu, G., Rossen, W. R., and Vincent-Bonnieu, S., Coreflood Study of Effect of Surfactant Concentration on Foam Generation in Porous Media. 2019, Ind. Eng. Chem. Res., 58, 1, 420-427

Nomenclature

Symbol	definition	Unit
CMC	critical micelle concentration	wt%
C_s	surfactant concentration	wt%
f_w	injected liquid volume fraction	-
f_g	foam quality	-
k	permeability	Darcy
PV	pore Volume	ml
u_t^{gen}	critical superficial velocity for foam generation	ft/day
u_t^{prop}	critical superficial velocity for foam propagation	ft/day
u_t^{col}	critical superficial velocity for foam collapse	ft/day
$\boldsymbol{\Phi}$	porosity	-
∇P^{min}	minimum pressure gradient	Pa/m
ΔP	pressure difference	bar
σ	surface tension	mN/m